RF characterisation of CMOS-compatible Silicon-on-Insulator Nanoelectromechanical Resonators

Yoshishige Tsuchiya[a], Naoaki Harada[a,b], Christos Giotis[a], Joshua Lamb[a], Faezeh Arab Hassani[a], Mitsuhiro Shikida[b], Cecilia Dupre[c], Eric Ollier[c], Sebastian T Bartsch[d], Adrian Mihai Ionescu[d], and Hiroshi Mizuta[a,e]

[a]Nanoelectronics and Nanotechnology Research Group, Department of Electronics and Computer Science, University of Southampton, Highfield Campus, Southampton SO17 1BJ, UK
[b]Department of Biomedical Information Sciences, Hiroshima City University, Hiroshima 731-3194, Japan
[c]CEA-LETI, MINATEC Campus, 38054 Grenoble Cedex 9, France
[d]Nanoelectronic Devices Laboratory, Ecole Polytechnique Fédérale de Lausanne, CH 1015 Lausanne, Switzerland
[e]School of Material Sciences, Japan Advanced Institute of Science and Technology (JAIST), Ishikawa 923-1292, Japan
e-mail: yt2@ecs.soton.ac.uk

Keywords: NEMS, Resonator, SOI, CMOS compatible

One of the recent trends of the researches on nanoelectromechanical (NEM) resonators is to investigate their possibilities of integration with advanced CMOS technology for active development of smart sensor systems with ultrasensitive NEM mass sensors and high-frequency NEM circuit components. Various NEM-based devices [1-3] and even NEM-resonator-integrated systems [4,5] have been reported in line with this trend. We have designed resonant-suspended-gate FET sensors and NEM resonator sensors on a SOI-CMOS compatible platform and analysed their characteristics both numerically and experimentally in [6]. However, further detailed understanding of their operational behavior would be very important to improve their performance for sensor and Radio-Frequency (RF) applications. In this paper, we have measured the resonance of the NEM resonators shown schematically in Fig. 1(a) in a systematic manner to discuss the mechanism behind their resonance behavior.

A schematic diagram of the device fabrication is shown in Fig. 1(b). The resonators are actually fabricated on the same wafer where advanced SOI-MOSFETs are fabricated concurrently. The source, drain, beam, and double side gates are uniformly heavily-doped in p-type with the boron doping concentration of 2.0 x 10^{18} cm^{-3}. This is beneficial for simplifying overall fabrication process. The initial SOI thickness is 45 nm and the designed beam length L_d and width W_d are varied. After oxidation, about 15-nm-thick SiO_2 has been grown surrounding the beam so that a Si-SiO_2 core-shell beam has been formed. An SEM image of a beam with L_d = 2 μm and W_d = 105 nm in between two side gates is shown in Fig. 1(c). In measuring the resonance of the beam, we have used frequency modulation (FM) in the lock-in current detection method. A schematic diagram of the measurement set-up is shown in Fig. 2. Electrical bias is only applied to the side gate 2, while the side gate 1 and back gate are grounded.

Figure 3 shows the in-phase current, X, measured in the lock-in amplifier as a function of the frequency for the beam with L_d = 1.5 μm and W_d = 105 nm. As the X is known to be proportional to the frequency derivative of the displacement of the beam [7], the observed peak at ~ 146.25 MHz at the RF power P = -15 dBm suggests a mechanical resonance. The quality factor Q of ~ 620 is consistent with the reported values for mechanical resonances [3]. The increase of the asymmetry of the line shape with increasing the RF power suggests strong nonlinearity of the resonance, which is also a characteristic feature of electromechanical resonators. In the modal analysis of this resonator, 161 MHz and 249 MHz are the 1st and 2nd eigenfrequencies, respectively. Therefore, the observed resonance would correspond to the 1st out-of-plain mode, suggesting that the out-of-plain oscillation whose displacement is perpendicular to the wafer plane has been excited by only controlling the bias of the in-plane side-gate electrode. Similar behavior has been confirmed for the resonators with various W_d. Misalignment between the beam and the in-plane side gates would be a possible reason. Figure 4 shows the resonance peak for the beam with L_d = 1 μm and W_d = 105 nm. The peak frequency of 215.2 MHz is significantly lower than the 1st eigenfrequency in simulation of 360 MHz. Effects of suspended edges of the anchor regions could explain this discrepancy. Figure 5 shows how the resonance is changed with respect to the side-gate voltage V_{sg2}. Fitted with the theoretical formula [7], the peak frequency, Q value and relative peak intensity are extracted as a function of V_{sg2} in Fig. 6 (a) and (b). Non-monotonous change of the resonance frequency with decreasing V_{sg2} suggests two competing effects, such as nonlinear hardening and electrostatic softening would take place in this voltage range.

In summary, we have investigated the resonance behavior of RF SOI NEM resonators with respect to the dimensions, gate biasing and RF power and found out (1) out-of-plain oscillation is able to be excited in this lay out, (2) effects of undercutting of the anchor on the resonance frequency are more serious to the shorter beam, and (3) effects of the side-gate bias on the out-of-plain oscillation are complicated and non-monotonous.

This work has been financially supported by EU FP7 project NEMSIC and by TOBITATE! Young Ambassador Program, MEXT, Japan. All data supporting this study are available from the University of Southampton repository at http://dx.doi.org/10.5258/SOTON/D0091.

References:
[1] C. Durand *et al.*, IEEE Electron Device Lett. 29, 494 (2008).
[2] D. Grogg *et al.* IEDM 2008 Tech. Dig., pp. 663.
[3] S. T. Bartsch *et al.*, IEDM 2012 Tech. Dig., pp. 351.
[4] E. Ollier *et al.*, Proc. MEMS 2012, pp. 1368
[5] A. Koumela *et al.*, Nanotechnology 24, 435203 (2013).
[6] F. Arab Hassani *et al.*, Sensors 13, 9364 (2013).
[7] V. Gouttenoire *et al.*, Small 6, 1060 (2010).

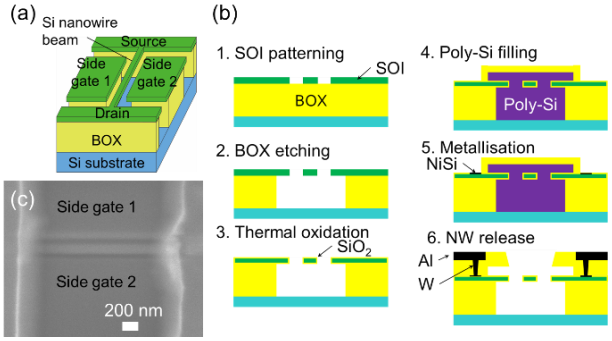

Figure 1. (a) A schematic drawing, (b) a typical fabrication process flow, and (c) an SEM image of the beam on an SOI NEM resonator.

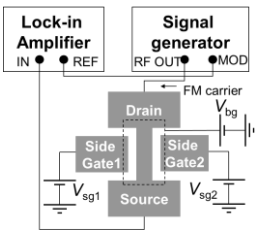

Figure 2. A schematic diagram of the lock-in current measurement system.

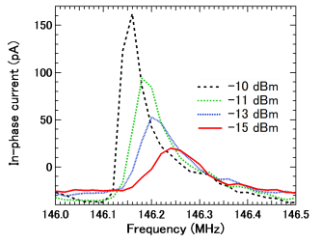

Figure 3. Change of the line shape of the resonance for 1.5-μm beam with respect to the RF power.

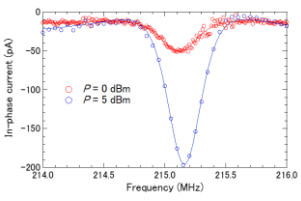

Figure 4. Resonance observed at 215.2MHz for the 1-μm beam.

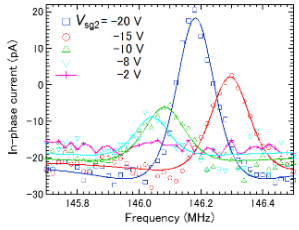

Figure 5. Resonance peak shift with applying negative V_{sg2}.

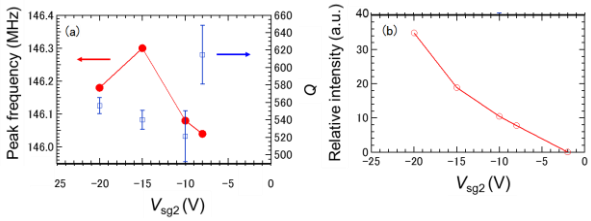

Figure 6. (a) Resonance frequency and Q value vs V_{sg2}. (b) Relative intensity as a function of V_{sg2}.